Mem. S.A.It. Vol. 79, 1271

Memorie della

Probing the emitting region using anomalous lensed QSOs

D.J.E. Floyd[1,2], N.F. Bate[2], and R.L. Webster[2]

[1] OCIW, Las Campanas Observatory, Casilla 601, Colina El Pino, La Serena, Chile
e-mail: dfloyd@lco.cl
[2] University of Melbourne, School of Physics, Parkville, Victoria 3010, Australia

Abstract. In gravitational lensing theory, it is predicted that two images which straddle a caustic will have the same magnification. However there are a significant number of well-observed cases where a factor of up to 10 is observed in the magnification ratio - "anomalous lensed quasars". These offer a unique window on the nature of both lens and lensed source: From recent modelling (Bate, Webster & Wyithe 2007; Congdon, Keeton & Osmer 2007) it appears that the size of the emission region convolved with the microlensing pattern is the main reason for the discrepancy. With appropriate modelling this can be turned around, and a measurement of the emission region of the quasar can be made. This is particularly interesting if a range of observations are made, either at different times (to more highly constrain the probability distribution) or in different wavebands (to constrain the size as a function of wavelength). We present recent multi-band observations of MG0414+0534 as a case study, demonstrating that the anomalous A2/A1 flux ratio decreases as we move blueward, and use the results to constrain the size of the r-band AGN emission region to < 7 light days.

Key words. gravitational lensing – accretion disks – quasars: individual (MG0414+0534)

1. Introduction

Lensed images are formed at positions where the optical path length is stationary - minima, maxima and saddle points of the Fermat travel-time surface (Fermats principle). Magnification, μ, due to a gravitational lens is determined by the total convergence κ_{tot} and the shear γ of the lens at these image locations: $\mu = \frac{1}{(1-\kappa_{tot})+\gamma][(1-\kappa_{tot})-\gamma]}$. Maxima and saddle points may exhibit demagnification, while minima are always magnified. In a quadruple system, the brightest image pair are found at a saddle point and a minimum. These images are typically magnified by a factor of $\sim 5-20$. As discussed in Schechter & Wambsganss (2002), the convergence κ_{tot} can be split into two components: smooth (κ_s), and compact ($\kappa_\star$). Compact material in the lens introduces small-scale perturbations in the lens potential (microlensing), producing new features in the Fermat travel-time surface, and hence in the magnification map – Fig. 1. Each macro-image saddlepoint or minimum contains a large number of micro-saddle points (one for each star in the lens). This has been found to explain the anomalous fluxes seen in some quasars (Witt, Mao & Schechter 1995).

Send offprint requests to: D. Floyd

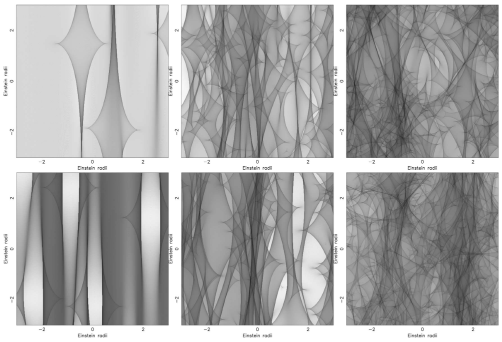

Fig. 1. Magnification maps showing the magnification with position for saddlepoint image (top) and minimum image (bottom). From left-to-right we have a clumpy matter content of 1%, 30% and 100% respectively. The uncrowded figure at top left clearly shows the basic shape of the caustic. Increased microlensing due to the clumpy lens matter produces a complicated Fermat travel-time surface and thus a magnification map made up of multiple overlapping caustics. Anomalous lensed quasars can occur when the saddlepoint image is only weakly magnified, but the minimum image magnified normally.

Dust (Lawrence et al. 1995) and millilensing by galactic substructure (Mao & Schneider 1998; Metcalf & Madau 2001; Chiba 2002; Dalal & Kochanek 2002) have also been explored as possible causes. However, millilensing should also affect the radio emission, for which an anomalous flux ratio is not observed.

Lensed quasars have been used before to place upper limits on the size of the emission region - most notably in Q2237+0305 (Witt, Mao & Schechter 1995; Wayth, ODowd & Webster 2005). Furthermore, it has been shown that changing the ratio of smooth to compact masses in the lens can produce anomalous flux ratios (Schechter & Wambsganss 2002). However, combining these two effects was only recently attempted (Bate, Webster & Wyithe 2007). Our new objective is to explore source size with wavelength and to explore this as a means of constraining the emission mechanism. Here we present preliminary results from our first test case, MG0414+0534.

Table 1. A2/A1 for MG0414+0534

Band	A2/A1
g'	< 0.20
r'	0.21 ± 0.1
i'	0.26 ± 0.1
z'	0.34 ± 0.1
J	0.60 ± 0.2
H	0.67 ± 0.2

2. Observations & fitting

We began this observational project using the Magellan telescopes in Nov. 2007. The aim is to get multi-band imaging of anomalous lensed QSOs in a single night using PANIC and IMACS or MagIC. We use short periods during nights with excellent seeing. Integration times are ~ 5 minutes per filter, (10 mins in the blue). There are six known anomalous quasars accessible from the south of which we have observed three. We fit astigmatism (A) and defocus (D) to the entire 30 arcmin IMACS field of view and produce a modified Gaussian PSF for the positions of the quasar images with an ellipticity and angle prescribed by the (A,D) pattern found. We use direct fitting of this PSF to each quasar image. We are experimenting with deconvolution techniques, using pre-existing HST images as models. MG0414+0534 was observed on 2007/11/18 & 2007/11/20 in $0\farcs5$ seeing – Fig. 2. This is our first test case, and A1 and A2 are only just resolved. However, it is clear that the A2/A1 ratio becomes more anomalous as we move blueward. In g, A2 is undetected.

3. Simulations & preliminary results

Microlensing simulations are conducted using a ray-shooting method (Kayser, Refsdal & Stabell 1986; Wambsganss et al. 1990). We allowed the smooth matter fraction in the lens to vary from 0 to 99% (see Bate et al. (2007) for full details). The model for MG0414+0534 is based on earlier work by Schechter & Wambsganss (2002). Fig. 3 illustrates the effect of source

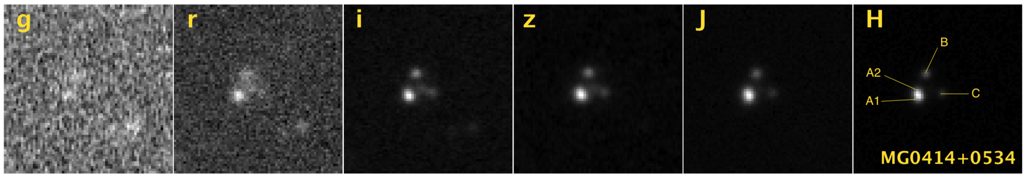

Fig. 2. Magellan IMACS + PANIC imaging of MG0414+0534 (November 2007). The anomalous flux ratio, A1/A2 increases as we move blueward.

size and lens model on the magnification probability distribution: Increasing the smoothness of the lens increases the relative probability of a low-magnification saddle point image (right columns in Fig. 3) and thus of an anomalous flux ratio. Increasing source size completely eliminates the flat low-magnification wing, making anomalous fluxes impossible.

We have now obtained imaging of sufficient quality to detect both members of an anomalous image pair of three anomalous lensed quasars. Data for MG0414+0534 has been modelled – table 1: It is clear that the A2/A1 ratio becomes more anomalous as we move blueward, consistent with a decreasing source size with decreasing wavelength. We fit the emitting region with a power law, $R = R_0(\frac{\lambda}{\lambda_0})^{\nu}$. Fig. 4 shows our combined probability distribution for the optical data (r, i, z) for MG0414+0534. Adding in the NIR data (in progress) will place stronger constraints on ν, and thus possible emission mechanisms in the very central region of this quasar. We can already constrain the size of the r-band to less than 0.5 lens Einstein radii. The other objects – observed May 2008 – are WFI 2026-4536 & SDSS J0924+0219. Both qualitatively show the same effect with the anomalous A2/A1 flux ratio visibly increasing with increasing wavelength (Floyd et al. in preparation), although the data have not yet been fully analysed.

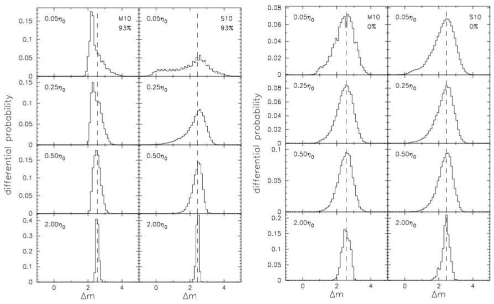

Fig. 3. Differential probability histograms for magnification in case of 93% smooth matter (left) and 0% smooth matter (right). Left and right columns correspond to the minimum and saddlepoint macromodels, respectively (both with $\mu = 10$). Source size (in Einstein radii, η_0) increases as we move down. Anomalous fluxes demand a nonzero probability of low magnification in the saddlepoint image.

4. Conclusions

For MG0414+0534, we place an 95% upper limit on the innermost r-band emission region of $1.9\times10^{14}h_{70}^{-1/2}(M/M_{\odot})^{1/2}$ metres, or roughly $7(h_{70}^{-1/2}(M/M\odot)^{1/2})$ light days. Analysis of the data is still under way (Bate, Floyd & Webster, in preparation), but we believe that this technique offers a powerful new way of probing

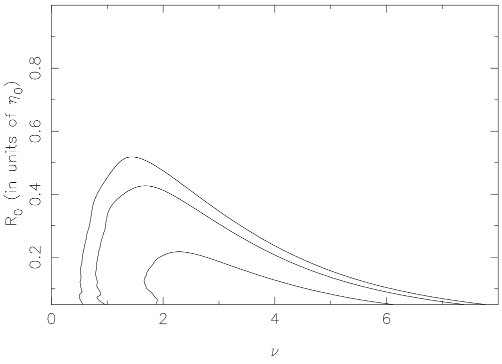

Fig. 4. Likelihood contours in spectral index, ν, and r-band source size, R_0 for MG0414+0534, using the optical data. The optical emission region is < 0.5 lens Einstein radii (95%).

the accretion mechanism in quasars, and constraining the size of the central emitting region.

Acknowledgements. We would particularly like to thank Joachim Wambsganss for the use of his ray-shooting code. DJEF acknowledges support of a Magellan fellowship from Astronomy Australia Limited. NFB acknowledges the support of an Australian Postgraduate Award.

References

Bate, N. F., Webster, R. L. & Wyithe, J. S. B. 2007, MNRAS, 381, 1591
Chiba, M. 2002, ApJ, 565, 17
Congdon, A. B., Keeton, C. R. & Osmer, S. J. 2007, MNRAS, 376, 434
Dalal, N. & Kochanek, C. S. 2002, ApJ, 572, 25
Kayser, R., Refsdal, S. & Stabell, R. 1986, A&A, 166, 36
Lawrence, C. R., Elston, R., Januzzi, B. T. & Turner, E. L. 1995, AJ, 110, 2570
Mao, S., & Schneider, P. 1998, MNRAS, 295, 587
Metcalf, R. B., & Madau, P. 2001, ApJ, 563, 9
Schechter, P. L. & Wambsganss, J. 2002, ApJ, 580, 685
Witt, H. J., Mao, S. & Schechter, P. L. 1995, ApJ, 443, 18
Wambsganss, J., Paczynski, B. & Katz, N. 1990, ApJ, 352, 407
Wayth, R. B., ODowd, M. & Webster, R. L. 2005, MNRAS, 359, 561